**Geomechanics and Engineering**, *Vol. 38, No. 2 (2024) 107-123*
https://doi.org/10.12989/gae.2024.38.2.107


# The effect of well inclination angle on sand production using FDM–FEM modelling; A case study: One of the oil fields in Iran

Nemat Nemati[1], Kamran Goshtasbi[2], Kaveh Ahangari*[1] and Reza Shirinabadi[3,4]

[1]*Department of Mining Engineering, Science and Research Branch, Islamic Azad University, Tehran, Iran*
[2]*Department of Mining Engineering, Faculty of Engineering, Tarbiat Modares University, Tehran, Iran*
[3]*Department of Petroleum and Mining Engineering, South Tehran Branch, Islamic Azad University, Tehran, Iran*
[4]*Research Center for Modeling and Optimization in Science and Engineering, South Tehran Branch, Islamic Azad University, Tehran, Iran*

(*Received January 10, 2022, Revised May 21, 2024, Accepted June 28, 2024*)

**Abstract.** The drilling angle of the well is an important factor that can affect the sand production process and make its destructive effects more severe or weaker. This study investigated the effect of different well angles on sand production for the Asmari Formation, located in one of the oil fields southwest of Iran. For this purpose, a finite difference model was developed for three types of vertical (90°), inclined (45°), and horizontal (0°) wells with casing and perforations in the direction of minimum and maximum horizontal stresses, then coupled with fluid flow. Here, finite element meshing was used, because the geometry of the model is so complex and the implementation of finite difference meshes is impossible or very difficult for such models. Using a combined FDM-FEM model with fluid flow, the sand production process in three different modes with different flow rates for the Asmari sandstone was investigated in this study. The results of numerical models show that the intensity of sand production is directly related to the in-situ stress state of the oil field and well drilling angle. Since the stress regime in the studied oil field is normal, the highest amount of produced sand was in inclined wells (especially wells drilled in the direction of minimum horizontal stress) and the lowest amount of sand production was related to vertical wellbore. Also, the Initiation time of sand production in inclined wells was much shorter than in other wellbores.

**Keywords:** numerical modeling; perforation; sand production; sanding initiation; sanding rate; well inclination angle

## 1. Introduction

Great challenges are faced by the industry in modeling sand production because it is a highly coupled hydro-mechanical process. To date, the continuum approach has been widely used in sand production experiments due to its simplicity, and mainly plasticity, mixture, or micromechanics theories have been utilized for model development. In this method, material behavior is analyzed as a continuous mass rather than as discrete particles, and it, therefore, cannot consider sudden changes or discontinuities. Detournay *et al.* (2006) used the approach to numerically quantify sand production. In their study, these researchers considered the existence of non-zero but reduced sand cohesions, and this was found to be more accurate than the zero cohesion assumption made by previous researchers. Although mechanical yielding and erosion models have been used to study sand production independently in most continuum models, a realistic sand production simulation needs an extensive coupling between the poro-mechanical and erosion models. A more reliable prediction approach for sand production has been shown by Detournay and Wu (2006) by coupling the poro-mechanical and erosion behaviors of the sanding formation. This study proposed two semi-analytical sand production models (SLAM and SPAM models) to simulate the disaggregation of the rock into the sand at shear failure (Mohr-Coulomb criterion) and the resulting sand production, which occurs with the fluid flow (Detournay and Wu 2006).

Wan *et al.* (2007), presented the extension of a finite element model of sand production based on erosional hydrodynamics to include a gas phase. A similar approach has been taken by Papamichos *et al.* (2001) and Papamichos and Malmanger (1999) combining the poro-mechanical behavior of the solid-fluid system with the erosion behavior of the solids due to fluid flow. These researchers developed finite element codes to simulate the non-linear coupling of the mechanical and erosion processes. Their model predicting sand production data was reasonably consistent with the measured sand production data. According to this model, the rock mass around a producing cavity needs to be mechanically failed by stress application to initiate the sanding process, and the sanding process will continue through the erosion process caused by the relatively weak hydrodynamic fluid flow forces (Papamichos *et al.* 2001, Papamichos and Furui 2013). Other continuous numerical models of the sand production process were developed, which are the basis of current continuous models.

A study of previous numerical models developed to simulate the sand production process shows that most models are two-dimensional and very simple and that three-dimensional models can not represent the complexity of

*Corresponding author, Dr.
E-mail: kaveh.ahangari@gmail.com

**Copyright © 2024 Techno-Press, Ltd.**
http://www.techno-press.org/?journal=gae&subpage=7
ISSN: 2005-307X (Print), 2092-6219 (Online)

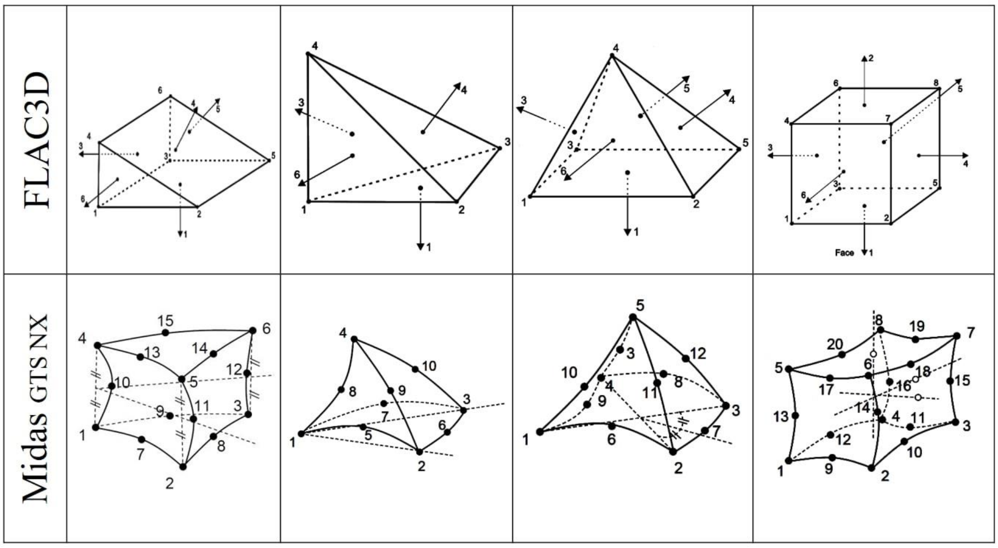


Fig. 1 The differences in structural features and numbering vertices between Midas and FLAC3D element shapes

well geometry with perforations. Many of these models are constructed as axisymmetric and only a limited section of well and formation is modeled. On the other hand, previous numerical models are designed only for vertical or horizontal wells. Therefore, simulation of the sand production process has not been done for inclined wellbores. Also, with these models, it is not possible to calculate the sand production rate accurately based on the production capacity of wells. As a result, an advanced three-dimensional numerical model is needed to display the complex geometry of well, perforations, and formation and study the sand production process more accurately.

## 2. Description of numerical modeling

### *2.1 Model construction*

In this study, a finite difference numerical model has been developed using FLAC3D 7.0 software to simulate the sand production process in one of the oil fields of Iran. The wellbores are modeled in three situations (5 positions in total): vertical (90°), inclined (45° in direction of minimum horizontal stress and maximum horizontal stress), and horizontal (0° in direction of minimum and maximum horizontal stresses). The final state of all wells is completed, cased, and perforated.

#### *2.1.1 Model meshing*

Since the geometry of wells with perforations is complex in the three situations mentioned above, therefore advanced meshing techniques are needed to simulate these conditions. The relatively simple meshing schemes in FLAC3D do not have the required capability to create such complex structures. Unlike finite difference meshing, finite element meshes have better flexibility in simulating complicated models. One of the available methods is to make the model in one of the finite element programs and after taking the output of the nodes and elements, transfer them to FLAC3D. In this regard, there are many finite element software such as ANSYS, PLAXIS, MIDAS, and ABAQUS that can save the nodes and elements of the built model as an output file after modeling. In this research, Midas GTS NX v.1.2 64bit, which is a geotechnical finite element software, is utilized to construct the model geometries and grid structures. Midas GTS NX is a simulation program developed for the evaluation of soil-structure interaction based on the finite element method. The types of meshing available in Midas include pyramid, tetrahedron, hexahedron, and hybrid (hexahedron + pyramid + tetrahedron) (Midas GTS NX 2019).

In this research, tetrahedron meshing has been used to simulate the well and the formation. Also, in sand simulation and erosion process, this type of meshing has a good performance. A code using fish was developed to convert the Midas meshes into FLAC3D meshes. This type of mesh minimizes stress and displacement discontinuities. The two software programs number the vertices of each shaped differently. Fig. 1 provides an example of the differences in structural features and numbering vertices between Midas and FLAC3D element shapes (Midas GTS NX 2019, Itasca Consulting Group 2021).

#### *2.1.2 Model geometry*

After integrating finite element meshing into the finite difference model, the coupled FDM - FEM model is now ready to simulate the sand production process. The formation's length, width, and height in this model are equal to 2.5×2.5×2.0 meters, respectively. The depth of the well in both vertical and horizontal directions is equal to 2.0 meters and in inclined direction is equal to 2.83 meters. The radius of the wellbore in all three modes is 0.1397 m (5.5 in). A hollow cylinder with a length of 2.0 m for vertical and horizontal wellbores and 2.83 m for inclined wellbores, an inner diameter of 0.216 m, and a thickness of approximately 3.0 cm has been modeled as a casing. The dimensions and mechanical specifications of the casing have been selected according to the standard of the American Petroleum

(a) vertical wellbore

(b) directional wellbore

(c) horizontal wellbore

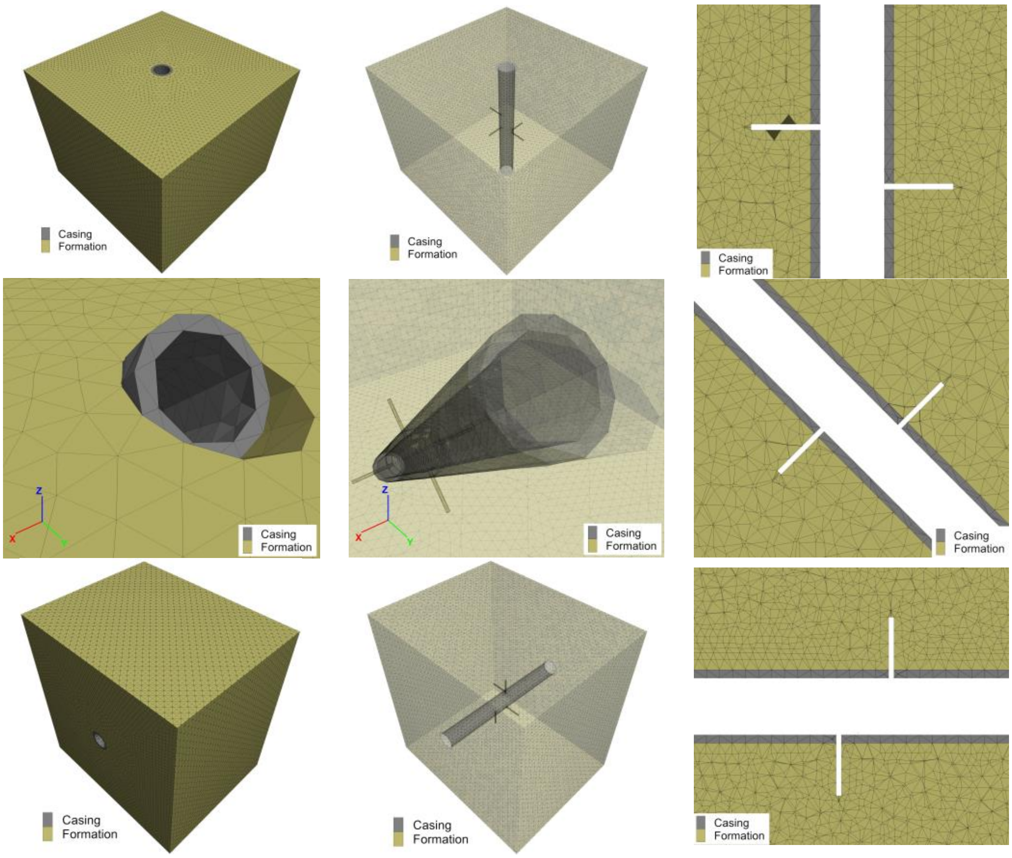


Fig. 2 The geometry of the formation, casing, and perforations in different situations of wellbore

Institute (API) (API 2012, Hansen 2018). In the middle of the casing, four perforations with a diameter of 2.0 cm are placed. The arrangement of perforations is diagonal and they are located at an angle of 90° to each other in the wall of the wellbore, therefore positioning each perforation in the direction of one of the horizontal stresses, makes it possible to check their situation by the stress changes. In all models, the depth of the perforations inside the formation reaches 35.0 cm.

Fig. 2 shows the basic geometry of the formation, wellbore, casing, and perforations in the FDM-FEM coupled model for different situations.

### *2.2 Boundary conditions and simulation steps*

After constructing the geometry of the model and assigning the initial and boundary conditions, it is time to run the model. As mentioned in the previous sections, sand production is related to the near-wellbore plastic strain state, which is determined by the local stress concentration. This requires the simulation of drilling, completion, and perforating phases before the simulation of the production phase to capture the correct stress and strain distributions around the wellbore (Volonté *et al.* 2013). In this research, the sand production modeling process has been carried out based on operational steps.

Boundary conditions are implemented in such a way that all grid points at the borders, corners, and edges of the model are fixed. In-situ vertical and horizontal stresses are also applied anisotropically to the model. The in-situ stress gradient is proportional to the depth of the reservoir relative to the ground surface. In Section 2, all data and information input to the software is completely arbitrary and is used only to evaluate the model and validation. Then the model runs.

For drilling the wellbore, a set of grid points is removed to simulate the drilling process (Feng *et al.* 2017). The boundary condition of the wellbore is such that all surfaces, including grid points located in the inner wall of the well, are free. The only intersection of the well with two upper and lower surfaces of the model (in both vertical and inclined situations) and two lateral surfaces (in horizontal mode) are fixed. These conditions allow the grid points inside the wall of the wellbore to move freely. A distributed load Pw with its magnitude equal to the drilling mud pressure is applied to the free wellbore surface. Then the model is solved until it reaches equilibrium.

In well completion step, a casing that was previously built in a finite element program is added to the model. Also, a certain space between the casing and formation is considered a cemented layer. The casing and cemented space around the well are fixed in place so that they do not displace and do not allow the wall of the wellbore to move. In the body of the casing, four cavities are pre-inserted as perforations and they are drilled into the formation from the continuation of these cavities. An additional set of elements, representing the perforations, are removed to simulate the perforating operation. After drilling the perforations, the

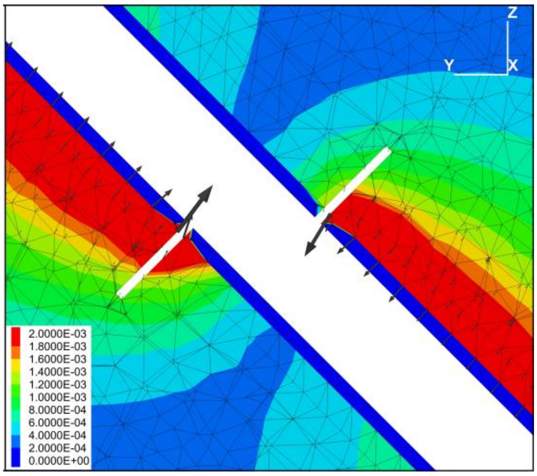


Fig. 3 Displacement curves and vectors around a hypothetical completed directional wellbore

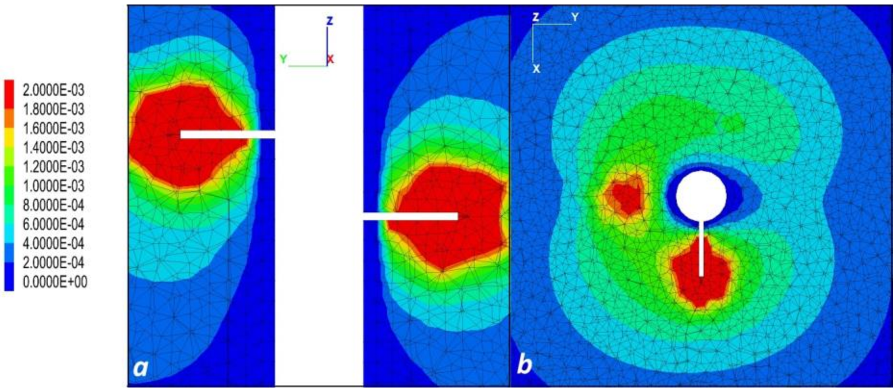


(a) A vertical section (b) A horizontal section

Fig. 4 Displacement curves in the presence of fluid flow

grid points on the free surfaces of the cavities are considered free, so that can move freely due to the stress redistribution or the influence of fluid flow.

It should be noted that in this modeling, the Mohr-Coulomb failure criterion was used for the reservoir sandstone. Elastic behavior is also considered for the casing. The behavior of the cement sheath is also selected similar to that of the sandstone. Fig. 3 shows an example of a completed assumptive directional well.

### 2.3 Applying fluid flow to the model

Because fluids tend to flow from high-pressure to low-pressure environments, fluid flow simulation has been performed for this model. In this way, the oil flow is directed from a high-pressure reservoir to the perforations and from there enters the wellbore environment. Because the main purpose of this modeling is to study the process of sand production and on the other hand all the wellbores are cased and completed, the flow path of the fluid has been chosen in the direction of perforations.

Fluid transport is mathematically modeled by Darcy's law. It is assumed that the amount of oil produced by a reservoir is uniform during its lifespan, and this is a simplifying condition in oil reservoir modeling which makes it possible to assume a constant production rate.

According to this theory, the fluid flow in the present model is considered isotropic. After assigning the parameters related to the fluid and applying the flow to the program, the model is run again to reach equilibrium in the presence of fluid flow. Fig. 4 shows the displacement curves in the model for a hypothetical well. As can be seen, the maximum displacement in the model is related to the end of the perforations, which has experienced stress redistribution due to the continuation of the fluid flow.

### 2.4 Simulation of the sand production process

So far, only fluid flow has been applied to the model. But a more efficient sand production simulation is required to complete the modeling process. Because FLAC3D is essentially a continuous software, it is not easy to calculate discontinuous parameters, such as instantaneous sand production, cumulative sand production, or sand production rate. Therefore, an advanced modeling technique is needed to measure the parameters of sand production. Using the sand criterion presented by Papamichos (1999, 2001, 2013), the points of the model that have been subjected to plastic yield due to the continuity of the fluid flow are determined. However, there are differences between the Papamichos criterion and the method used in this study in how to find critical points. The tips of the perforations are mainly

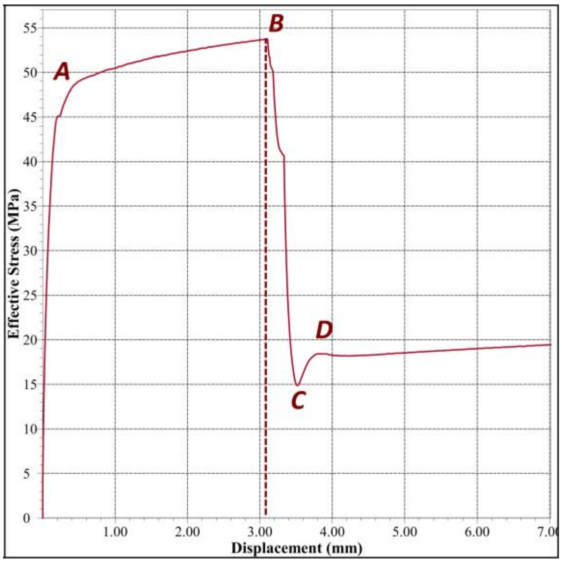


Fig. 5 The effective stress-displacement curve corresponds to a gridpoint at the end of a perforation

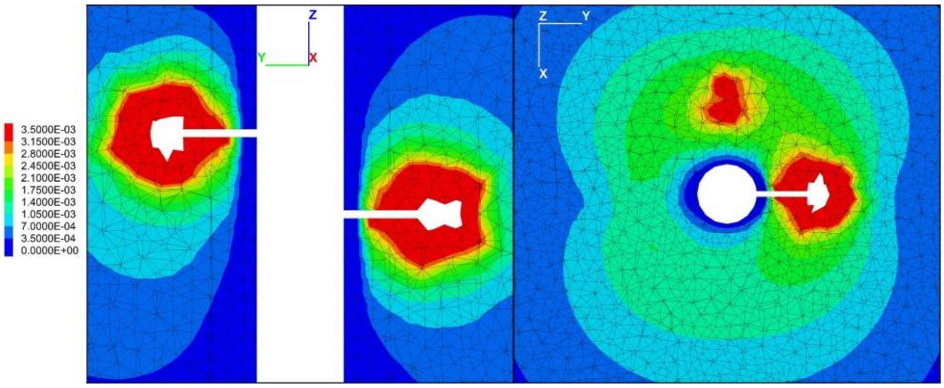


Fig. 6 The final shape of perforations, after producing sand and removing the yielded zones from the model

affected by the maximum amount of plastic strain (Fig. 4). Therefore, during the analysis, a grid point at the end of one of the perforations is selected and then the effective stress-strain or effective stress-displacement curve for that point is plotted by FLAC3D. In the obtained diagram, where the effective stress curve suddenly drops, it shows that the sandstone has yielded at that point and the amount of displacement corresponding to that, is considered as the critical displacement. Then, any gridpoint whose displacement value is equal to or greater than the critical displacement will be removed from the model. The weight values of the grid points removed from the model will indicate the amount of sand produced from the reservoir.

Fig. 5 shows the effective stress-displacement curve for sandstone at the end of one of the perforations in a hypothetical model is plotted by FLAC3D. As can be seen, the effective stress values are ascending from point A to B. This indicates an increase in the strength of sandstone in proportion to the increase in destructive forces caused by the fluid flow. When the curve reaches point B, it experiences a sudden drop in the amount of effective stress until it reaches point C with a steep slope. This indicates that the sandstone has yielded at point B and cannot withstand effective stresses beyond that point. Thus point B (i.e., 53.5 MPa) shows the Maximum strength of the formation sandstone against the fluid flow forces. The curve then reaches point D from point C with a lower slope.

Since the sandstone has lost a significant amount of its resistance, so if the fluid flow continues, the strength of the sandstone cannot exceed point D. Then, as the fluid continues to flow, the effective stress from point D increases with a gentler slope. so that the sand yields again at another point. The dashed line drawn from point B shows the corresponding displacement magnitude. This value is, in fact, the critical displacement. That is, displacements equal to or greater than this, indicate the degradation of sand grains. In this example, according to the diagram, the value of the critical displacement is equal to 3.10 mm. In this step, the program will remove gridpoints from the model that have a displacement equal to or greater than the critical value. Fig. 6 shows the final state of perforations in a vertical wellbore with a production flow of 1,200 barrels per day. As can be seen, the program automatically deletes gridpoints with a displacement equal to or greater than 3.10 mm.

### *2.5 Model validation*

In this section, stress and displacement distributions around a wellbore in an elasto-plastic (non-porous) medium obtained from the numerical model are compared with those calculated from analytical solutions. A wellbore subjected to a constant inner wellbore pressure and a uniform far-field stress is considered. The formation is assumed to be a linear-elastic and perfect-plastic material with a yield surface defined by the Mohr-Coulomb criterion. For this problem, the radial distance R0 of the yield zone is given by (Salençon 1969)

$$R_0 = r_w \left( \frac{2}{K_p + 1} \cdot \frac{P_0 + \frac{q}{K_p - 1}}{P_i + \frac{q}{K_p - 1}} \right)^{\frac{1}{K_p - 1}} \tag{1}$$

Where

$$K_p = \frac{1 + sin(\varphi)}{1 - sin(\varphi)} \tag{2}$$

$$q = 2C \times \tan\left(45 + \frac{\varphi}{2}\right) \tag{3}$$

$r_w$ is the wellbore radius, $P_0$ is the uniform far-field stress, $P_i$ is the wellbore pressure, φ is the friction angle and C is the cohesion strength. The stresses and radial displacement in the plastic zone ($r \le R_0$) can be expressed as

$$\sigma_r = -\frac{q}{K_p - 1} + \left(P_i + \frac{q}{K_p - 1}\right)\left(\frac{r}{r_w}\right)^{K_p - 1} \tag{4}$$

$$\sigma_\theta = -\frac{q}{K_p - 1} + K_p \left(P_i + \frac{q}{K_p - 1}\right)\left(\frac{r}{r_w}\right)^{K_p - 1} \tag{5}$$

$$u_r = \frac{r}{2G}\left[(2\nu - 1)\left(P_0 + \frac{q}{K_p - 1}\right) + \frac{(1-\nu)(K_p^2 - 1)}{K_p + K_{ps}}\left(P_i + \frac{q}{K_p - 1}\right)\left(\frac{R_0}{r_w}\right)^{K_p - 1}\left(\frac{R_0}{r}\right)^{K_{ps}+1} + \left(\frac{(1-\nu)(K_pK_{ps} + 1)}{K_p + K_{ps}} - \nu\right)\left(P_i + \frac{q}{K_p - 1}\right)\left(\frac{R_0}{r_w}\right)^{K_p - 1}\right] \tag{6}$$

Where

$$K_{ps} = \frac{1 + \sin(\psi)}{1 - \sin(\psi)} \tag{7}$$

G is the shear modulus, ν is the Poisson's ratio and ψ is the dilation angle. The stresses and radial displacement in the elastic zone ($r \ge R_0$) can be expressed as

$$\sigma_r = P_0 - \left(P_0 - \frac{2P_0 - q}{K_p + 1}\right)\left(\frac{R_0}{r}\right)^2 \tag{8}$$

$$\sigma_\theta = P_0 + \left(P_0 - \frac{2P_0 - q}{K_p + 1}\right)\left(\frac{R_0}{r}\right)^2 \tag{9}$$

$$u_r = \frac{R_0^2}{2G}\left(P_0 - \frac{2P_0 - q}{K_p + 1}\right) \cdot \frac{1}{r} \tag{10}$$

Table 1 Input data for validation of elastoplasticity model

| Parameters | Values | Units |
|---|---|---|
| Young Modulus (E) | 11.26 | GPa |
| Shear Modulus (G) | 7.69 | GPa |
| Poisson's Ratio (ν) | 0.306 | - |
| Cohesion Strength (C) | 13.795 | MPa |
| Friction Angle (φ) | 34.634 | Deg. |
| Dilation Angle (ψ) | 30.0 | Deg. |
| In-situ Stresses ($P_0$) | 55.0 | MPa |
| Mud pressure ($P_i$) | 30.4257 | MPa |

Here, using the data in Table 1, the numerical model constructed for three types of vertical, horizontal, and directional wellbores have been validated in comparison with the analytical method. Figs. 7 and 8, show the comparisons of near-wellbore stresses and displacement calculated from the analytical solution and the numerical model, respectively for three types of vertical, inclined, and horizontal wells.

As can be seen, the results demonstrate a very good agreement, verifying the reliability of the presented numerical model on modeling elasto-plastic material behaviors for all three types of wellbores. In addition, the maximum amount of radial displacement is related to inclined wells and the minimum is related to horizontal wellbores.

## 3. Case study

In this section, the numerical model introduced in the previous section is used to simulate the sand production process in wells located in one of Iran's oil fields. The oil field of this study is located in the southwest of Iran, which is characterized by a very gentle N-S to NE-SW trending anticline in the South-East, and a NW-SE trending fold in the North-East (Abdollahie Fard *et al.* 2006). Its structure belongs to the stable shelf of the Arabian Platform and there are limited geological outcrops from subsurface structures that can be evaluated on the surface (Berberian 1995). This field is one of the richest petroleum systems in the Middle East, having Gurpi, Kazhdumi, and Gadvan source rocks and Asmari, Fahliyan, and Khami/Bangestan reservoirs. Field data obtained from this structure have revealed unconformities and erosional surfaces due to the uplifting of basement horsts.

The reservoir studied in this oil field is located in Asmari Formation and is known as Asmari Reservoir. This reservoir includes alternating layers of dolomite, limestone, anhydrite, sandstone, and shale. The infiltration of sandstones into southwestern Iran has continued throughout the Asmari cycle. In terms of sedimentary environment, sandstones are divided into the lower part (Eocene-Oligocene) and upper part (Early Miocene). At the end of the Oligocene and the Miocene boundary, a general advance covers most parts of the Zagros Basin, resulting in a shallow carbonate environment throughout that area. This environment has been infiltrated from the southwestern and northern regions of the Persian Gulf by sands that have interfered with deep limestones towards the southwestern regions of Iran (Alavi 2004).

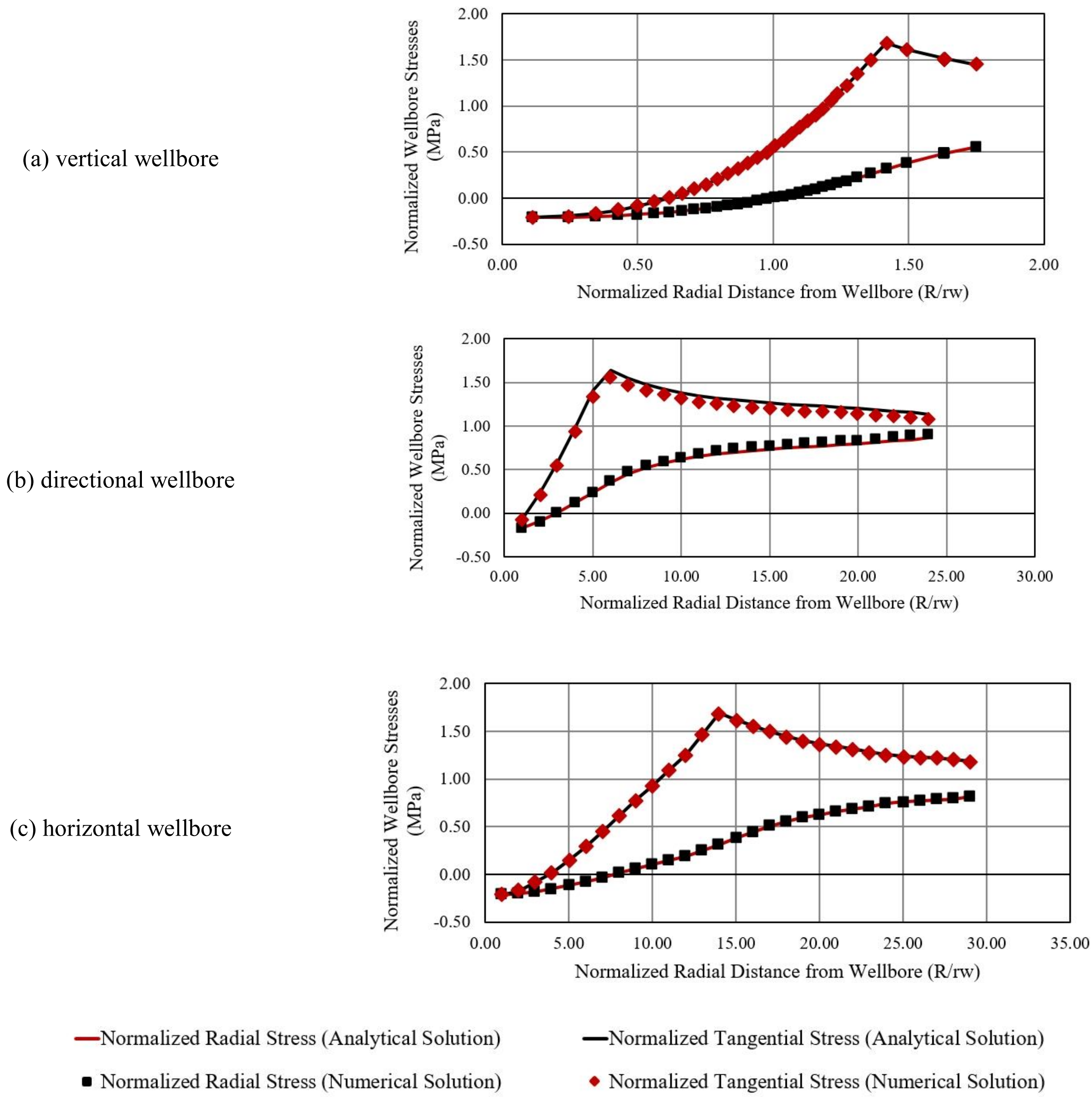


Fig. 7 Comparison of radial and tangential stresses along with the normalized radial distance from analytical solution and numerical model for different situations

In this oil field, the rock type in the Asmari reservoir is mainly sandstone, and its mechanical properties decrease significantly as the depth increases. Based on this, the exploitation of this oil field, especially at greater depths, is associated with significant sand production. Therefore, oil companies have to spend a lot of money every year to control the sand and compensate for the damages caused by it. Therefore, in this research, it is possible to study the sand production process for different angles of wells located in this oil field by presenting a numerical coupled model.

## 4. Simulation results and discussions

To simulate and investigate the effect of well inclination angle on the sand production process in the Asmari reservoir, the numerical model presented in this research is used. This numerical method described above provides a new and unique method of simulating sand production and erosion of perforations in different wells during production. Another unique feature of this model is the calculation of sand production rate in terms of the production flow of wells. So far, most numerical models have measured the rate of sand production based on parameters such as pore pressure, drawdown pressure, or formation pressure. However, since in industry, the optimal flow rate to prevent the production of sand (without the implementation of mechanical systems) is of particular importance, so in this model, according to the values of sand production rate, different flows can be compared with each other and selected the optimal production flow. In this section, by performing extensive sensitivity analysis on different well

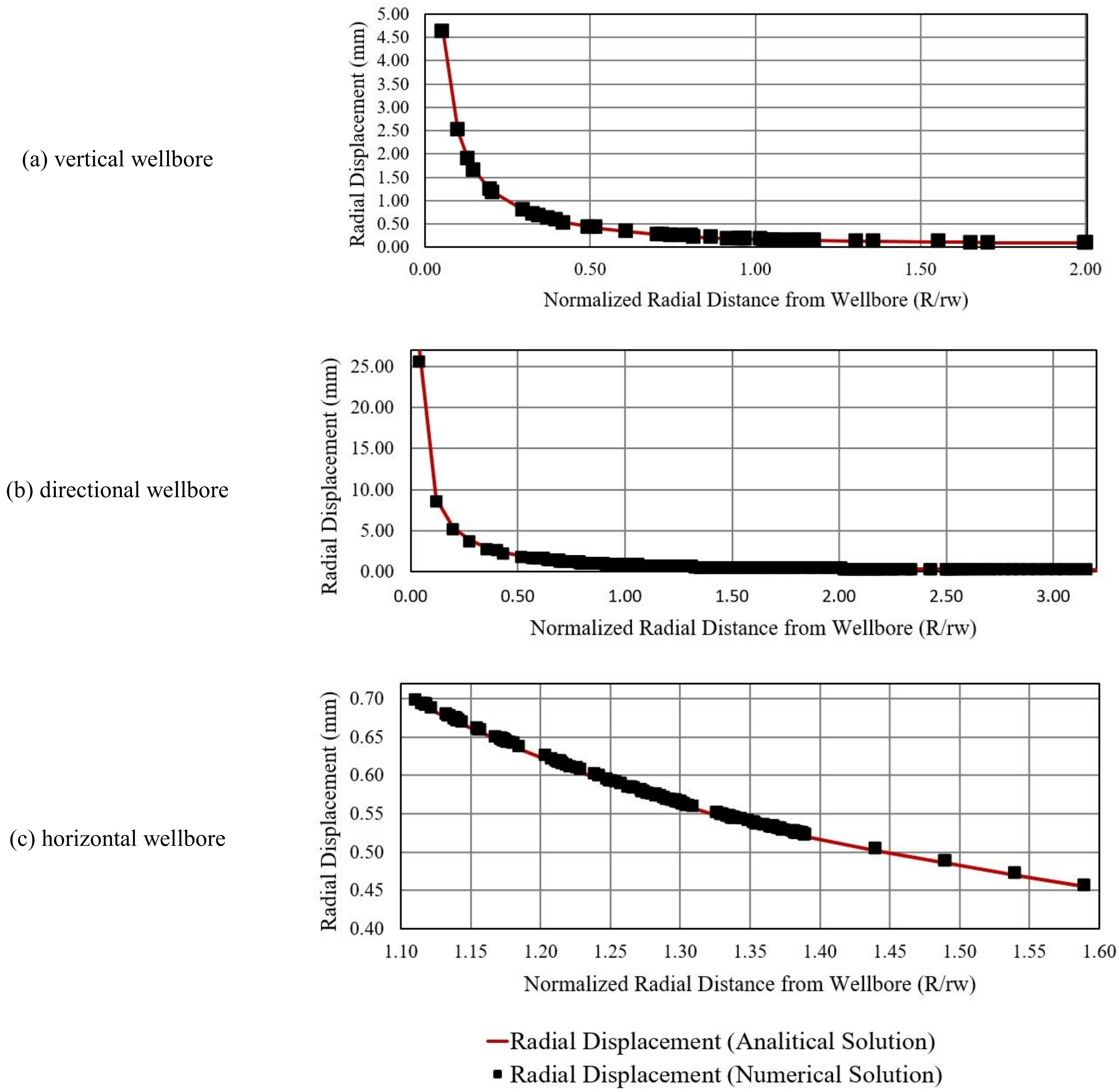


Fig. 8 Comparison of radial displacement along with the normalized radial distance from analytical solution and numerical model for different situations

conditions in the studied oil field, acceptable results have been obtained.

### *4.1 Estimation of input parameters*

In this section, the input parameters required to apply the proposed numerical model are estimated using the well and field data. These parameters consist of the mechanical parameters and strength of rocks as well as the pore pressure, in-situ stresses, etc. Characterizations of the geomechanical parameters were started by estimates of elastic parameters (i.e., Young's modulus and Poisson's ratio) using laboratory statical tests and dynamic-elastic formulations. Table 2 shows the simulation parameters used in the wellbores model. It should be noted that all the data used in the model were the same for all modes (i.e., vertical, horizontal, and inclined).

### *4.2 Simulating process*

To investigate of the different conditions of sand production in the Asmari reservoir of the oil field mentioned above, several oil wells have been studied. All of these wells have faced the problem of producing sand and even in some of them, oil production from the Asmari reservoir has been stopped due to the high amount of sand produced. The wells studied in this research are vertical, inclined, and horizontal. Because the effects of horizontal stresses on inclined and horizontal wellbores are greater, these wellbores are modeled in two directions of minimum

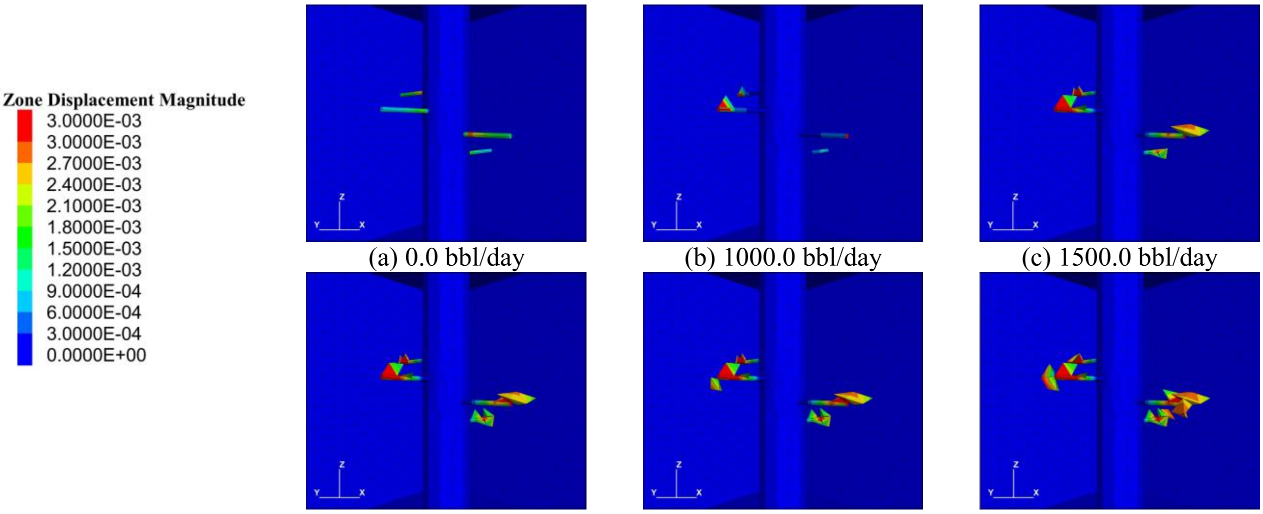


(a) 0.0 bbl/day (b) 1000.0 bbl/day (c) 1500.0 bbl/day

(d) 2000.0 bbl/day (e) 2500.0 bbl/day (f) 3000.0 bbl/day

Fig. 9 The final state of the perforations in a vertical well with different flow rates

Table 2 Simulation parameters were used for the wellbore models

| Parameters (Symbol) | Values | Units |
|---|---|---|
| Vertical Stress ($\sigma_v$) | 71.25 | MPa |
| Maximum Horizontal Stress ($\sigma_H$) | 53.11 | MPa |
| Minimum Horizontal Stress ($\sigma_h$) | 47.42 | MPa |
| The density of Rock ($\rho_r$) | 2270 | kg/m$^3$ |
| Young's Modulus of Rock ($E_r$) | 9.60 | GPa |
| Shear Modulus (G) | 3.78 | GPa |
| Bulk Modulus (K) | 6.956 | GPa |
| Tensile Strength ($\sigma_t$) | 2.30 | MPa |
| Cohesion Strength (C) | 5.485 | MPa |
| Friction Angle ($\varphi$) | 39.0 | ( °) |
| The density of Casing ($\rho_c$) | 7850.0 | kg/m$^3$ |
| Young's Modulus of Casing ($E_c$) | 210.0 | GPa |
| Poisson's Ratio of Casing ($\nu_c$) | 0.3 | - |
| The density of Fluid ($\rho_f$) | 840.0 | kg/m$^3$ |
| Pore Pressure ($P_p$) | 27.924 | MPa |
| Permeability (k) | 9.0 | mD |
| Porosity (n) | 0.23 | - |

and maximum horizontal stress.

It is noteworthy that in this oil field, the measurement of the sand production rate in the wells with the problem has not been done. But according to the field reports, most of these wells, with a flow rate of 1,000 to 1,500 barrels per day do not have a problem in terms of sand production and with a flow of 2,000 barrels per day, they are on the threshold of producing sand (regardless of the water produced). Although Ghalambor *et al.* (1989) and Veeken *et al.* (1991) have considered the allowable sand production rate for wells that continuously produce sand, between 6.0 and 600.0 grams per cubic meter, in this study, based on the reports of the operational engineers, according to the special conditions of the oil field, this amount is considered equal to 1.0 gr/m$^3$. Hence, according to the field report, it is assumed that wells that do not have a problem with sand production with a flow of 1,000 to 1,500 barrels per day, their average sand production rate has been less than 1.0 gram per cubic meter, and wells with a daily flow of more than 2,000 barrels also produce more than 1.0 gram per cubic meter of sand. The numerical model was calibrated on this basis.

The modeling procedure is similar to the methods presented in Section 2. Using the data in Table 2, modeling is performed for vertical, horizontal, and inclined states in the directions of minimum and maximum horizontal stresses (5 modes in total). In this model, the Mohr-Coulomb failure criterion is used. It should be noted that in the stage of fluid production and sand erosion, the analysis continues until no more sand is produced or the rate of sand production reaches a constant trend. Upon reaching such a state, the analysis stops.

#### *4.2.1 Vertical wellbores*

Simulation of the sand production process for a vertical well with flows of 1000, 1500, 2000, 2500, and 3000 barrels per day was performed using the data in Table 2. Fig. 9 shows the final state of the perforations after analysis. As can be seen, the amount of sand production increases with increasing well production flow. In the vertical well, in all different states of flow, the sand production rate in perforations excavated in the direction of minimum horizontal stress (X-axis) was higher than other perforations.

Fig. 10 shows a diagram of cumulative sand production versus time and at different flow conditions. This diagram shows 600.0 seconds of analysis. As expected, the higher the flow of the well, the higher the mass of sand produced.

As can be seen, for flows of less than 2,000 barrels per day, the mass of produced sand increases and slowly reaches a constant value after a while. But for flows of more than 2,000 barrels per day, first, the mass of produced sand increases rapidly, afterward the graph gradually decreases and then converges to a constant value. The reason for the increase in sand production rate is the plastic deformation of the perforations, which after a while, due to the appearance of new surfaces and their greater relative strength compared to previous surfaces, the sand production

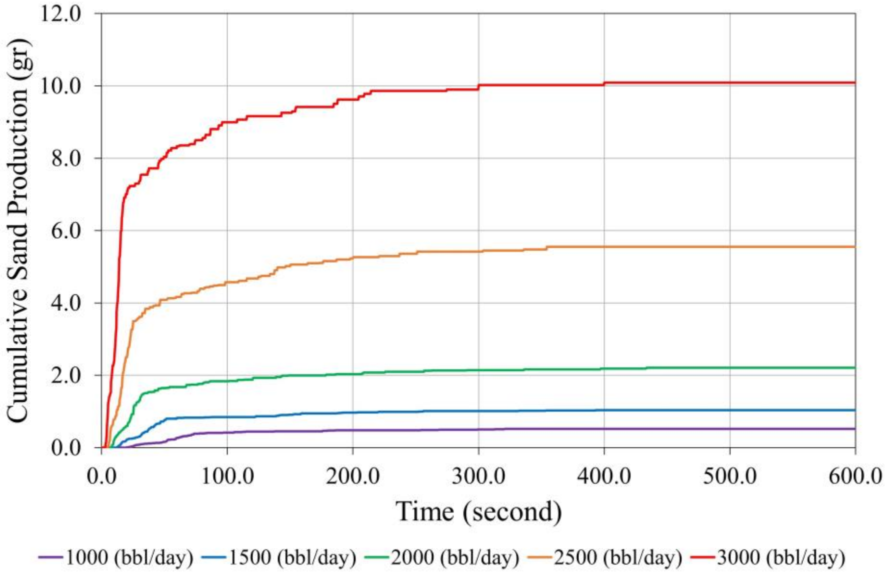


Fig. 10 Cumulative sand production versus time in a vertical wellbore

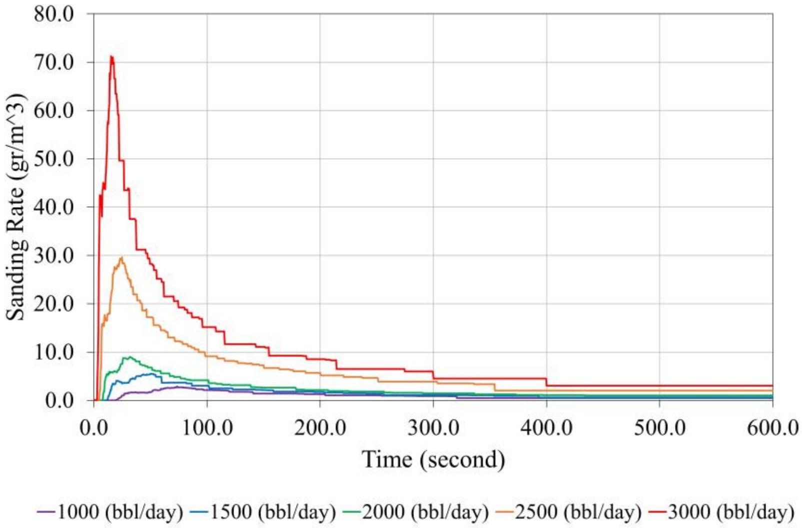


Fig. 11 Sand production rate versus time in a vertical wellbore

process decreases and then remains constant. The diagram of sand production rate versus time for 600.0 seconds of analysis is also shown in Fig. 11. In this figure, after 600 seconds, the sand production rate curves have found a stable state. In all curves, a peak point is observed after a moment. These points represent transient sand production in the well. As mentioned above, as the degraded sand particles are removed by the fluid flow, new rocks appear around the cavities and it takes some time for these sections to fail. This causes the mass of produced sand and as a result, the sand production rate to decrease, until the curve of the sand production rate remains constant at a certain value.

#### *4.2.2 Inclined wellbores*

Inclined wellbores were modeled and analyzed in two directions of minimum and maximum horizontal stresses. Figs. 12-15 show the results of the analysis of the sand production process for an inclined well drilled in different directions of horizontal stresses. As can be seen in the figures, the amount of sand produced in inclined wellbores is much higher than in vertical wells.

In general, inclined wells, due to their special position in the depths, are affected by all three vertical, minimum, and maximum horizontal stresses. According to Fig. 3, if the magnitude of stresses is high, the wall of an inclined well may be subjected to bending, and as a result, in the center of gravity of the well, the stress concentration is created and then the well is destroyed (Morita 2004). On the other hand, in the previous sections, it was shown that the maximum amount of radial displacement is related to inclined wellbores. Therefore, under normal conditions, an inclined well may be exposed to the maximum amount of plastic strain and become unstable. Fluid flow, as a destructive factor, can also exacerbate the critical condition of an

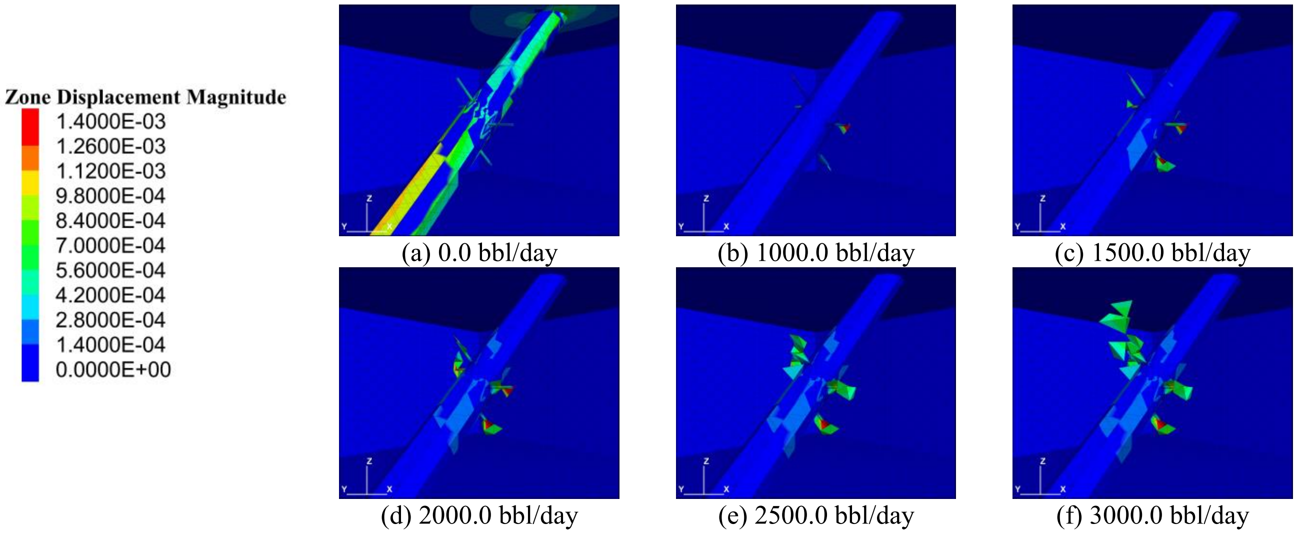


Fig. 12 The final state of perforations in an inclined well drilled in the direction of minimum horizontal stress, with different flow rates

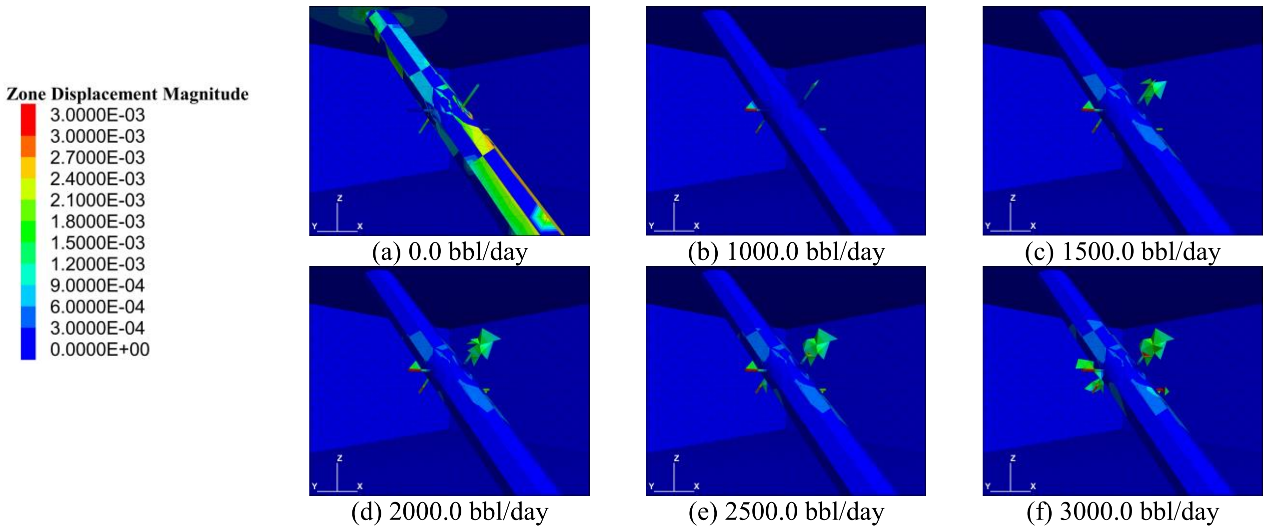


Fig. 13 The final state of perforations in a deviated well drilled in the direction of maximum horizontal stress, with different flow rates

inclined well. This is also true for perforations. Because in this situation, the perforations are oblique, the amount of stress concentration and plastic deformation around the perforations of inclined wells is more than other wellbores. In such cases, if fluid flow enters the perforations, the matrix will break and the sand grains will be easily separated.

Also, comparing the results of inclined wells with each other (e.g., Figs. 14 and 15), it can be seen that the amount of sand produced in the inclined well drilled in the direction of minimum horizontal stress is more than the inclined well that drilled in the direction of maximum horizontal stress. Because the first well is located in the minimum horizontal stress field, so the stress concentration in perforations is also higher.

Another important parameter that should not be neglected is the type of reservoir stress regime. According to the data in Table 2 and the state of stresses, it can be understood that in the Asmari reservoir of the studied oil field, the stress regime is of the normal type. Therefore, due to the high intensity of vertical and one of the horizontal stresses in the normal faulting regime, the perforations of an inclined well are strongly affected by stresses, and if this well is drilled in the direction of minimum horizontal stress, the highest amount of sand production will be related to this well. This condition has also been reported in studies by Al-Ajmi (2006), Al-Ajmi and Zimmerman (2006a, b, c), and Al-Shaaibi *et al.* (2013). As can be seen in Figs. 14 and 15, in this type of wellbore, the curves have reached a stable state after 1500 seconds of analysis.

### *4.2.3 Horizontal Wellbores*

Similar to inclined wells, horizontal wellbores were also modeled and analyzed in two directions of minimum and maximum horizontal stress. Figs. 16-19 are related to the results of the analysis of a horizontal wellbore drilled in different directions of horizontal stresses. As shown in the figures, under the same conditions, the amount of sand

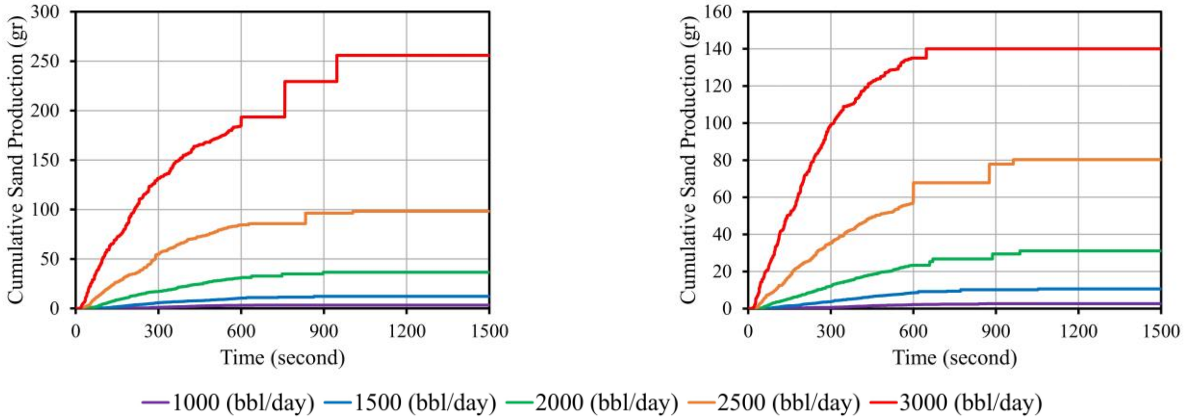


(a) In the direction of $\sigma_h$ (b) In the direction of $\sigma_H$

Fig. 14 Cumulative sand production versus time in an inclined wellbore drilled in different directions

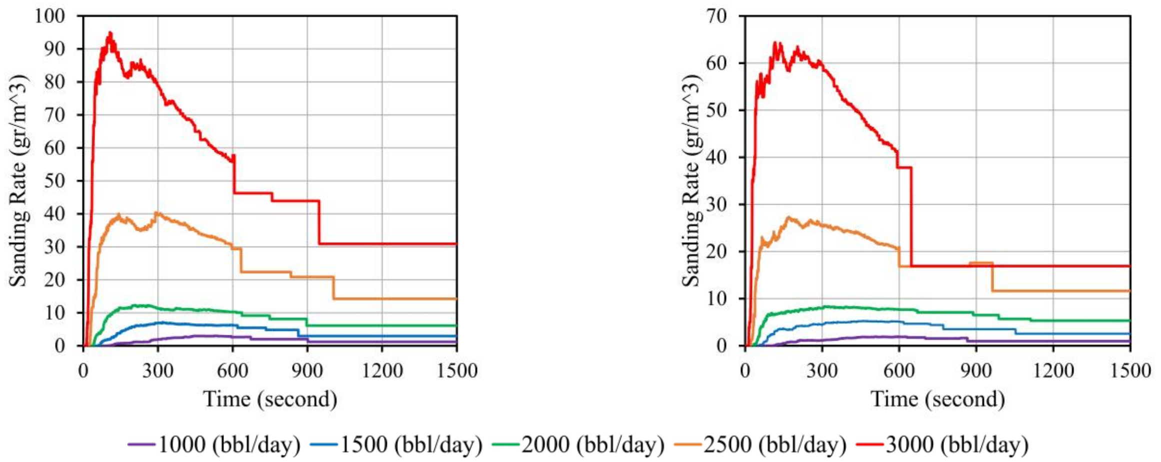


(a) In the direction of $\sigma_h$ (b) In the direction of $\sigma_H$

Fig. 15 Sanding rate versus time in an inclined wellbore drilled in different directions

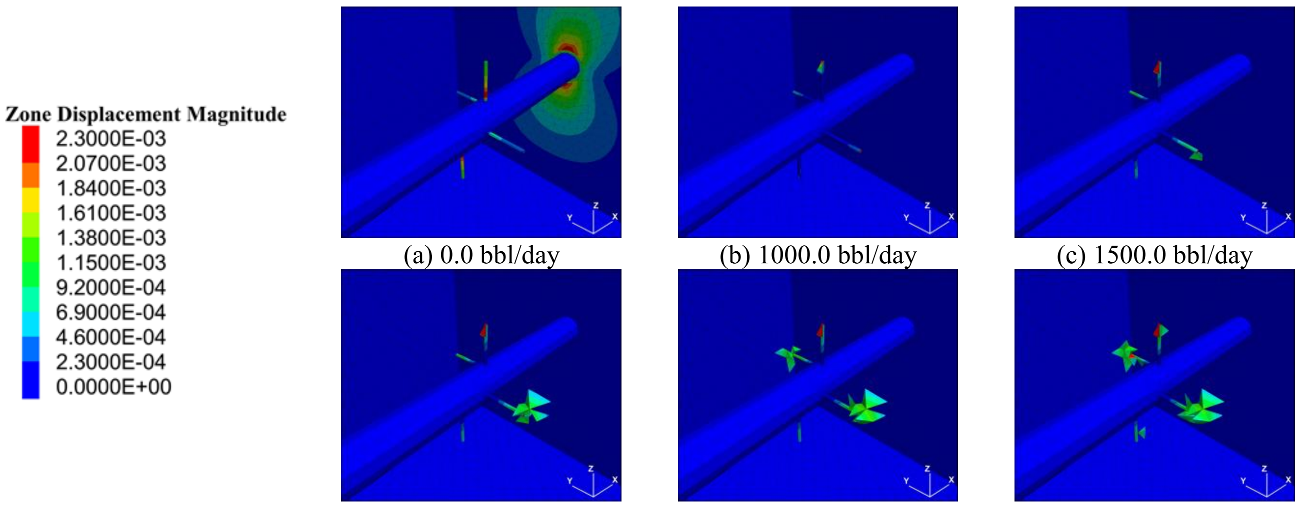


(a) 0.0 bbl/day (b) 1000.0 bbl/day (c) 1500.0 bbl/day

(d) 2000.0 bbl/day (e) 2500.0 bbl/day (f) 3000.0 bbl/day

Fig. 16 The final state of perforations in a horizontal well drilled in the direction of minimum horizontal stress, with different flow rates

produced in horizontal wells is less than the amount produced in inclined, and it is more than in vertical wellbores. According to Figs. 18 and 19, in the model of horizontal wells, the trend of the curves has been fixed after 1200 seconds of analysis.

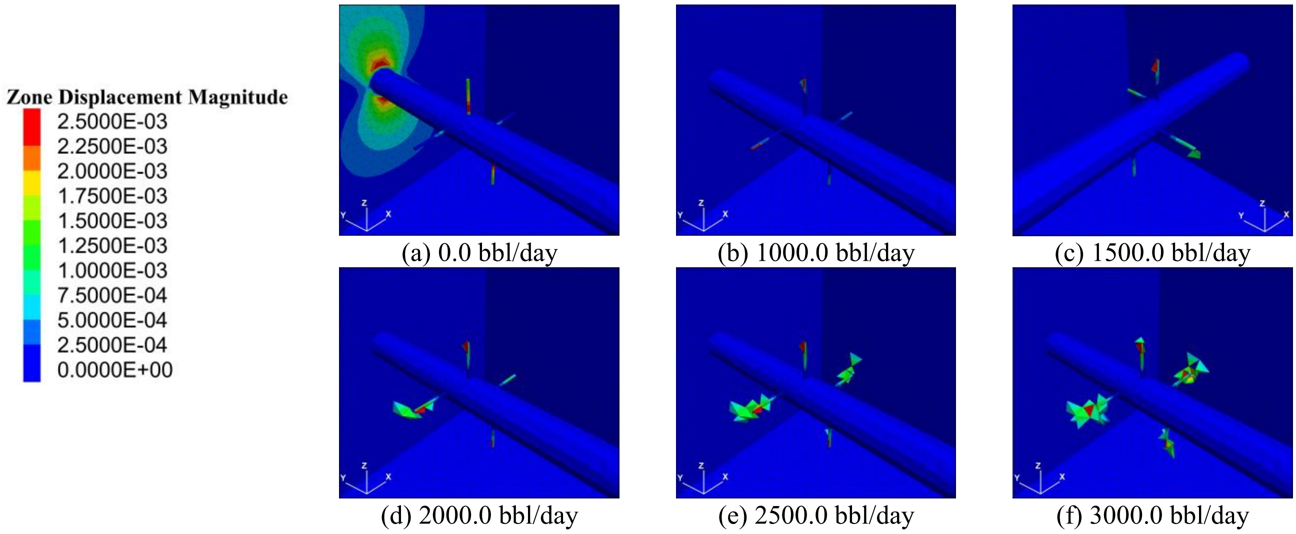


Fig. 17 The final state of perforations in a horizontal well drilled in the direction of maximum horizontal stress, with different flow rates

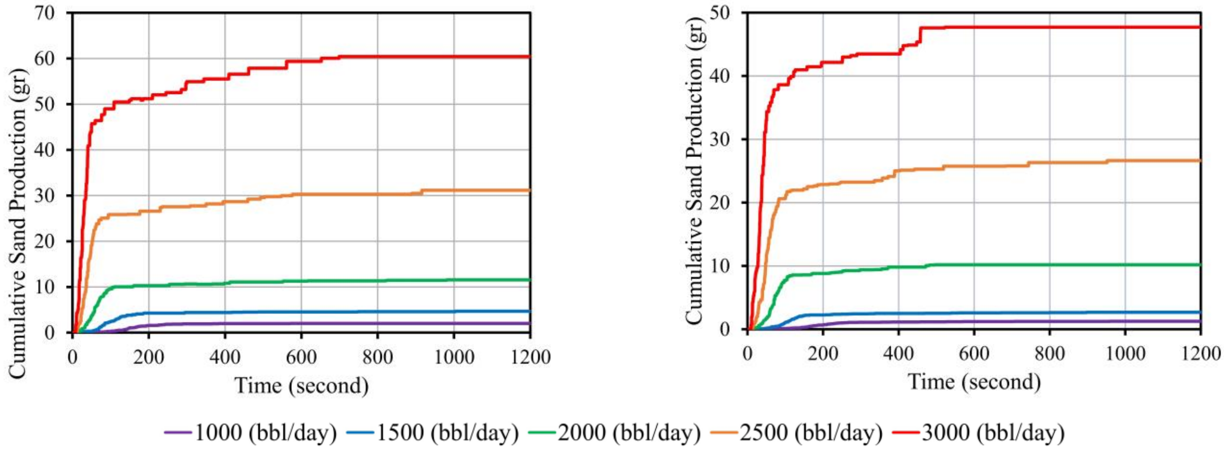


(a) In the direction of $\sigma_h$ (b) In the direction of $\sigma_H$

Fig. 18 Cumulative sand production versus time in a horizontal wellbore drilled in different directions

In this modeling, compared to inclined wells, because horizontal wells are completely drilled in line with one of the horizontal in-situ stresses, they are less exposed to stress. Therefore, the stress concentration in horizontal wells and perforations is less than that of inclined wells. The same issue causes the sand production rate in horizontal wells to be less intense than in inclined wells. Also, among the horizontal wellbores, that drilled in the direction of minimum horizontal stress produced less sand than another horizontal well. Cavities of the horizontal well drilled in the direction of the minimum horizontal stress are mainly in the direction of the vertical and maximum horizontal stresses, which will result in the highest stress concentration and, as a result, plastic shear strain at those points. This causes an increase in the sand production rate in the horizontal well drilled in the direction of the minimum horizontal stress compared to those drilled in the direction of the maximum horizontal stress. The numerical results obtained in the model presented in this research are consistent with the study of Al-Shaaibi *et al.* (2013).

### *4.3 Comparison of results*

In this section, the results obtained from different wellbore conditions are compared. Fig. 20 shows a diagram of the sanding initiation in terms of different well flows. As can be seen, as the flow of the well increases, sand is produced in a shorter period. This condition exists in all curves. However, with the increasing flow in inclined wellbores, sand is produced faster than in vertical and horizontal wells. Although the sand is produced in inclined wells in a shorter period than other wells, as can be seen, the difference in the direction of the inclined wellbores does not have a significant effect on the sanding initiation. On the other hand, the longest time to start producing sand is related to the vertical well. This reason can be seen as the lower effective stress in the wall of the vertical well compared to the other two types of wellbores and as a result, the reduction of the stress concentration in this well compared to the others.

Fig. 21 shows a graph of cumulative sand production in different wells concerning different flow rates for the analysis

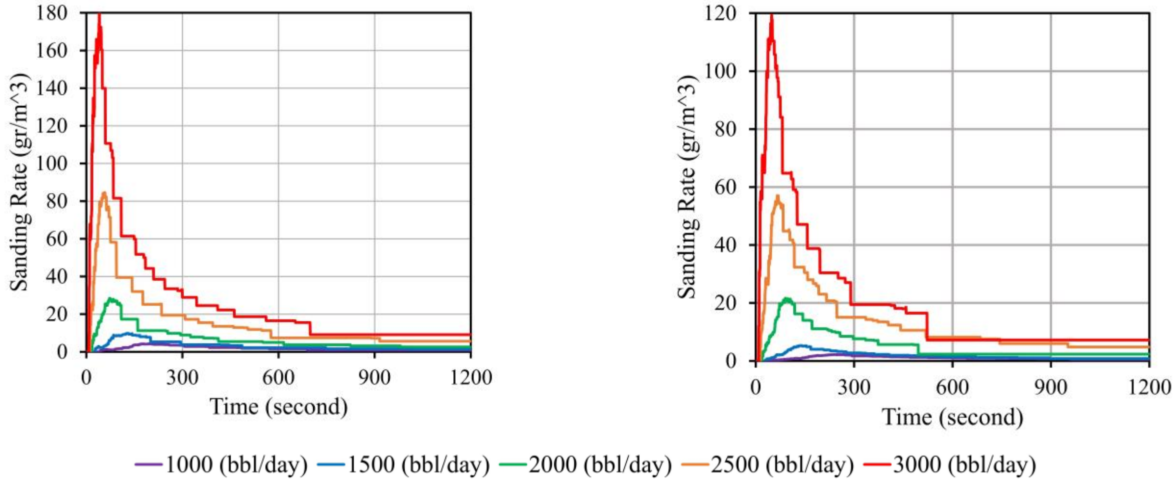


(a) In the direction of $\sigma_h$ (b) In the direction of $\sigma_H$

Fig. 19 Sanding rate versus time in a horizontal wellbore drilled in different directions

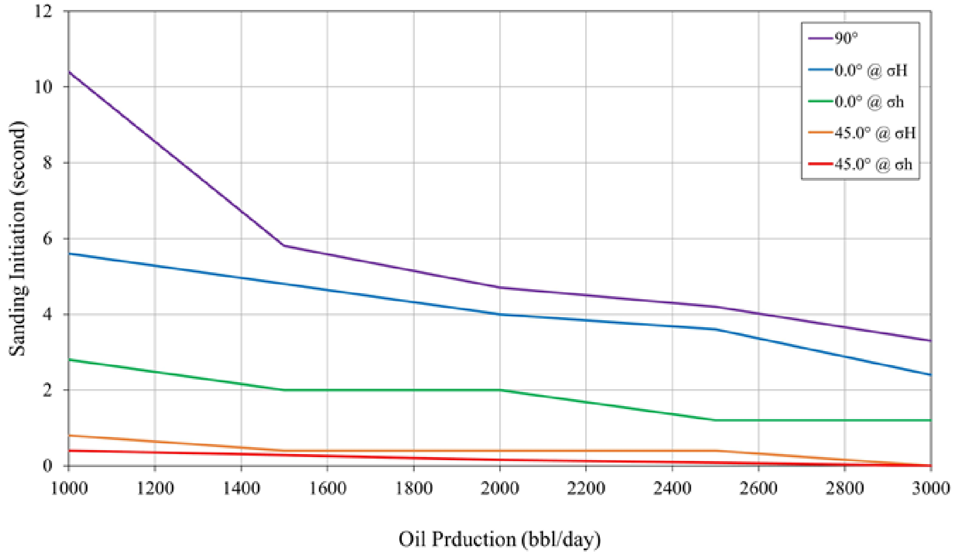


Fig. 20 Sanding initiation in terms of different well flows20 Sanding initiation in terms of different well flows

period. According to this diagram, the inclined well drilled in the direction of minimum horizontal stress produced the highest amount of sand. While the lowest amount of produced sand is related to vertical wells. In horizontal and inclined wells, sand is produced at a relatively uniform rate as the well flow increases. However, after the flow exceeds a certain amount, the intensity of sand production suddenly increases. For example, in an inclined well drilled in the direction of minimum horizontal stress, the sand production process accelerates by increasing the well flow from 2000 barrels per day. Meanwhile, in the horizontal wells, with the increase of 2500 barrels per day, the production of sand becomes more intense. But in vertical wellbore, these changes is almost uniform.

Fig. 22 also shows a diagram of the maximum rate of sand production relative to the well flow for different modes. Due to this figure, the rate of sand production increases in all wells in proportion to the increased flow rate. But in inclined wellbores, this process occurs more intensely. As can be seen in the diagram, the vertical well produces sand at a much lower rate as the flow increases. Also, there is not much difference between the rate of sand production in horizontal wells drilled in the direction of minimum or maximum horizontal stresses. While the difference in sand production rate is greater in inclined wells. For example, in an inclined wellbore with a daily production of 2,500 barrels per day, if drilled in the direction of minimum horizontal stress, the sand production rate is 14.2367 grams per cubic meter and if drilled in the direction of maximum horizontal stress, it's sand production rate will be 10.6381 gr/m$^3$. In other words, in this oil field, depending on whether the inclined wellbore with a flow rate of 2,500 barrels per day is drilled in the direction of minimum horizontal stress or maximum horizontal stress, the difference in sand production rate will be equal to 3.5986 grams per cubic meter. While this difference is only 0.820 gr/m$^3$ for horizontal wells.

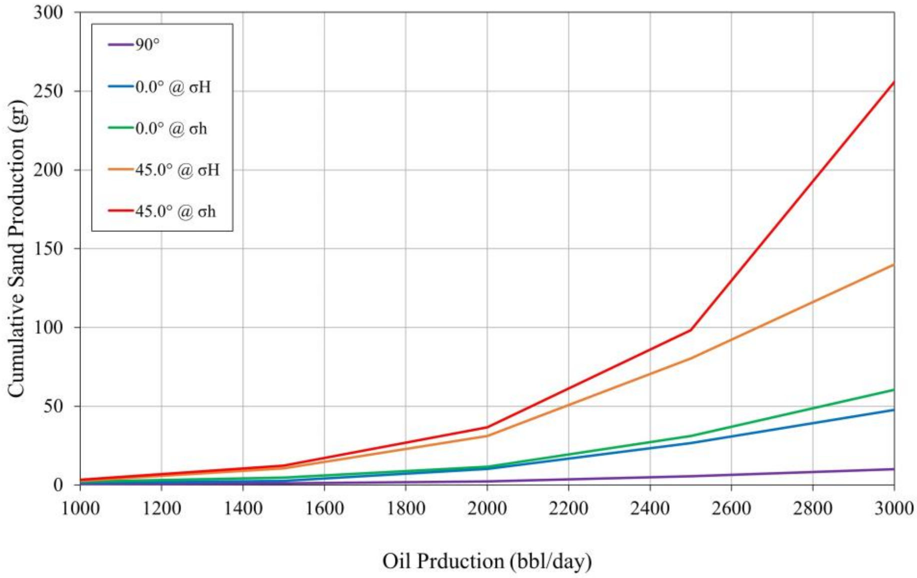


Fig. 21 Cumulative sand production in different wells concerning different flows for the analysis period

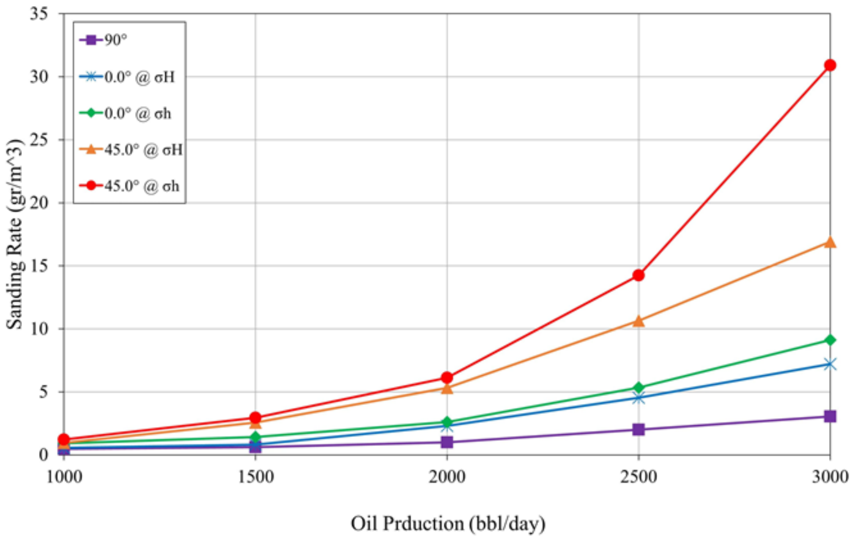


Fig. 22 Sanding rate in terms of different well flows

As mentioned above, the fault regime of the reservoir is of normal type. Based on Al-Shaaibi *et al.* (2013), in a normal stress regime with anisotropic horizontal stresses, the vertical borehole is more stable than the horizontal and deviated borehole in all directions. In normal stress regimes, the vertical stress is greater than the maximum horizontal stress. As a result, vertical boreholes are more stable than horizontal and deviated boreholes in all directions (Al-Shaaibi *et al.* 2013). Because the vertical wells are drilled in the direction of maximum stress (vertical stress), as a result, the cavities are mainly located in the direction of minimum and maximum horizontal stresses. Unlike cavities in horizontal wells, which are subjected to vertical stress and one of the horizontal stresses. In other words, some cavities are placed in the direction of vertical stress in any position of the horizontal well (either in the direction of the minimum or maximum horizontal stress), so the stress concentration in the wall of these wellbores is higher. It causes an increase in the sand production rate compared to the vertical well. In inclined wells, due to the position of the wellbore and perforations, the cavities are simultaneously exposed to all three types of vertical and minimum and maximum horizontal stresses. Therefore, in the normal stress regime, the lowest sand production rate is related to the vertical well due to the low stress concentration, and due to the high concentration of stress and the increase in plastic shear strain, the highest sand production rate is also related to inclined wells.

According to this modeling and with the permissible rate of 1.0 grams per cubic meter for sand production, in this oil field, vertical wells with a maximum flow rate of 2,000 barrels per day, horizontal wells with a flow rate of 1,350-1,600 barrels per day, and inclined wells with a flow rate of 750-1,100 barrels per day will not have a problem with sand production. In addition, the best model of the wellbore in this oil field (according to the normal stress regime) is the vertical well and the worst-case scenario is for inclined wells (especially wells drilled in the direction of minimum horizontal stress). It is recommended that inclined wellbores not be perforated as much as possible in this oil field. Because in addition to the instability of the well, it will lead to the highest amount of sand production. If necessary, it is better to use sand prevention systems such as gravel packs. In the case of horizontal wells, the wellbore pressure should be adjusted so that horizontal stresses (especially minimum horizontal stress) do not affect the stability of the well and perforations.

Since no measures have been taken to estimate the sand production rate in the wells located in the studied oil field, therefore the numerical model introduced in this research and the values obtained from it have not been calibrated with field conditions. It is recommended that when using this modeling method, to obtain more accurate and reliable results, the initial model should first be calibrated with the reservoir conditions in terms of sand production.

It should be noted that in this study, the analyses were performed in a continuum-based model and since sand production is inherently a discontinuum process, it is better to use a discontinuum-based numerical method (or a combination of continuum-discontinuum numerical models) to achieve more accurate results.

## 5. Conclusions

In this study, to investigate the effect of well inclination angle on sand production, a finite difference-finite element coupled model was constructed. Then this numerical model was used to simulate the sand production process in the Asmari reservoir of one of the oil fields located southwest of Iran. Wellbore models were designed for 5 modes: vertical, inclined in the direction of $\sigma h$, inclined in the direction of $\sigma H$, horizontal in the direction of $\sigma h$, and horizontal in the direction of $\sigma H$. In this model, for the first time, a new model of sand erosion was used to calculate sand production parameters. After performing the analysis, the following results were obtained:

- Due to the normal stress regime in the field, the highest amount of produced sand was related to inclined wells.
- Among the inclined wells, the one drilled in the direction of minimum horizontal stress, produced the highest amount of sand.
- In inclined wellbores, the direction of in situ stresses does not significantly affect the onset of sand production.
- The lowest amount of sand was produced from vertical wells.
- In horizontal wellbores, the direction of in situ stresses does not have much effect on the amount of produced sand.
- Well-path optimization is mainly controlled by the magnitude of the in-situ stresses and the reservoir stress regime.

## Acknowledgments

The authors wish to thank the National Iranian South Oil Company (NISOC) for this work's technical information and financial support. The authors also appreciate Christine Detournay for providing one of her valuable studies to complement the scientific information in this research.

## References

Abdollahie Fard, I., Braathen, A., Mokhtari, M. and Alavi, S.A. (2006), “Interaction of the Zagros Fold Thrust Belt and the Arabian-type, deep-seated folds in the Abadan Plain and the Dezful Embayment, SW Iran”, *Petroleum Geosci*., **12**(4), 347-362. https://doi.org/10.1144/1354-079305-706.

Al-Ajmi, A.M. (2006), “Wellbore stability analysis based on a new true-triaxial failure criterion”, Ph.D. Dissertation, Royal Institute of Technology, Stockholm.

Al-Ajmi, A.M. and Zimmerman, R.W. (2006a), “A New 3D stability model for the design of non-vertical wellbores”, The 41st U.S. Symposium on Rock Mechanics (USRMS), Golden, Colorado, June.

Al-Ajmi, A.M. and Zimmerman, R.W. (2006b), “Stability analysis of deviated boreholes using the Mogi-Coulomb failure criterion, with applications to some oil and gas reservoirs”, *Proceedings of the IADC/SPE Asia Pacific Drilling Technology Conference and Exhibition*, Bangkok, Thailand, November. https://doi.org/10.2118/104035-MS.

Al-Ajmi, A.M. and Zimmerman, R.W. (2006c), “Stability analysis of vertical boreholes using the Mogi–Coulomb failure criterion”, *Int. J. Rock Mech. Min. Sci*., **43**(8), 1200-1211. https://doi.org/10.1016/j.ijrmms.2006.04.001.

Alavi, M. (2004), “Regional stratigraphy of the Zagros fold-thrust belt of Iran and its proforeland evolution”, *Am. J. Sci*., **304**(1), 1-20. https://doi.org/10.2475/ajs.304.1.1.

Al-Shaaibi, Sh.K., Al-Ajmi, A.M. and Al-Wahaibi, Y. (2013), “Three dimensional modeling for predicting sand production”, *J. Petroleum Sci. Eng*., **109**, 348-363. https://doi.org/10.1016/j.petrol.2013.04.015.

API Specification (2012), 5CT, ISO 11960:2011, Petroleum and natural gas industries - Steel pipes for use as casing or tubing for wells, American Petroleum Institute (Purchasing Guidelines); USA.

Berberian, M. (1995), “Master "blind" thrust faults hidden under the Zagros folds: active basement tectonics and surface morphotectonics”, *Tectonophysics*, **241**(3-4), 193-224. https://doi.org/10.1016/0040-1951(94)00185-C.

Detournay, C. and Wu, B. (2006), “Semi-analytical models for predicting the amount and rate of sand production”, Multiphysics Coupling and Long Term Behaviour in Rock Mechanics – Van Cotthem, Charlier, Thimus & Tshibangu (eds), Taylor & Francis Group, London. https://doi.org/10.1201/9781439833469.ch53.

Feng, Y., Li, X. and Gray, K.E. (2017), “Development of a 3D numerical model for quantifying fluid-driven interface debonding of an injector well”, *Int. J. Greenhouse Gas Control*, **62**, 76-90. https://doi.org/10.1016/j.ijggc.2017.04.008.

Ghalambor, A., Hayatdavoudi, A., Alcocer, C.F. and Koliba R.J. (1989), “Predicting sand production in U.S. gulf coast gas wells producing free water”, *J. Petroleum Technol*., **41**(12), 1336-1343. https://doi.org/10.2118/17147-PA.

Hansen, B. (2018), Production casing design considerations, Devon Energy Corporation (NYSE: DVN), Oklahoma City, Oklahoma, USA. www.devonenergy.com.

Itasca Consulting Group, Inc. (2021), User's Manual of FLAC3D (Fast Lagrangian Analysis of Continua in 3-Dimensions), Version 7.0, Minneapolis, Minnesota USA. www.itascacg.org.

Midas GTS NX v. 1.2 (2019), User's Manual of MIDAS G.T.S. N.X. (GeoTechnical analysis System–New eXperience) Software, Midasoft Inc., New York, NY, USA. https://www.midasoft.com/geo/gtsnx/products/midasgtsnx.

Morita, N. (2004), "Well orientation effect on borehole stability", *Proceedings of the SPE Annual Technical Conference and Exhibition*, Houston, Texas, USA. September, https://doi.org/10.2118/89896-MS.

Papamichos, E. and Malmanger, E.M. (1999), "A sand erosion model for volumetric sand predictions in a North Sea reservoir", *SPE Reservoir Eval. Eng.*, **4**(1), 42-50, https://doi.org/10.2118/69841-PA.

Papamichos, E., Vardoulakis, I., Tronvoll, J. and Skjvrstein, A. (2001), "Volumetric sand production model and experiment", *Int. J. Numer Anal. Method. Geomech.*, **25**(8), 789-808. https://doi.org/10.1002/nag.154.

Papamichos, E. and Furui, K. (2013), "Sand production initiation criteria and their validation", *Proceedings of the 47th U.S. Rock Mechanics/Geomechanics Symposium*, San Francisco, California, USA, June.

Salençon, J. (1969), "Contraction quasi-statique d'une cavité à symétrie sphérique ou cylindrique dans un milieu élasto-plastique", Annales des Ponts et Chaussées, **4**, 231-236.

Veeken, C.A.M., Davies, D.R., Kanter, C.J. and Kooijman, A.P. (1991), "Sand production prediction review: Developing an integrated approach", *Proceedings of the SPE Annual Technical Conference and Exhibition*, Dallas, Texas, USA, October. https://doi.org/10.2118/22792-MS.

Volonté, G., Scarfato, F. and Brignoli, M. (2013), "Sand prediction: A practical finite-element 3D approach for real field applications", SPE Production and Operations, 28(01), 95-108, https://doi.org/10.2118/134464-PA.

Wan, R.G., Liu, Y. and Wang, J. (2007), "A multiphase flow approach to modeling sand production using finite elements", J. Can. Petroleum Technol., **46**(4), 40-46, https://doi.org/10.2118/07-04-04.

Wang, J., Yale, D. and Dasari, G. (2011), "Numerical Modeling of Massive Sand Production", SPE Annual Technical Conference and Exhibition, Denver, Colorado, USA, October, https://doi.org/10.2118/147110-MS.

Wang, J. and Papamichos, E. (2012), "Sand Production by Different Criteria and a Validation by a Perforated Test in a Sandstone", SPE Heavy Oil Conference Canada, Calgary, Alberta, Canada, June, https://doi.org/10.2118/158255-MS.

*CC*